

Progress at CENAM to Develop a Cs Fountain Frequency Standard

J. M. López-Romero, S. López-López, E. de Carlos-López, N. Shtin, F. Jiménez-Tapia

Centro Nacional de Metrología
km 4,5 Carretera a Los Cués, 76246, Querétaro, México.
mauricio.lopez@cenam.mx

ABSTRACT

The Centro Nacional de Metrología, CENAM, is currently developing a Cs fountain primary frequency standard, which is referred as CsF-1, with the aim to experimentally realize the unit of time with an uncertainty of parts in 10^{15} or better. Currently, the Magneto-Optical Trapp (MOT) of the CsF-1 is under routinely operation, its characterization has been done as function of its operational parameters. When writing this article the vacuum tube of the flight region is under construction. A threefold magnetic shielding has been designed and constructed. Sapphire oscillators to be used as local oscillator at the CsF-1 have been also designed, assembled and characterized.

1. INTRODUCTION

Since 1998 the CENAM Time and Frequency Division started to design and develop Cesium atomic clocks. The first developed Cs clock was a non commercial optically pumped thermal Cs frequency standard, named CsOp-1. Evaluation of the major systematic frequency shifts on the CsOP-1 was reported in [1]. Currently the CsOP-1 is under major changes to improve its accuracy [2] to be around 3×10^{-14} . During 2002 year CENAM began the development of a Cs fountain clock [3] with the aim to experimentally realize the unit of time with an uncertainty of parts in 10^{15} or better. Currently the Cs fountain clock at CENAM presents an advanced state on its development and it is near to be completed. Currently, the Magneto-Optical Trapp (MOT) of the CsF-1 is under routinely operation, its characterization has been done as function of its operational parameters [4]. When writing this article the vacuum tube of the flight region is under construction. A threefold magnetic shielding has been designed and constructed. Sapphire oscillators to be used as local oscillators at the CsF-1 have been also designed, assembled and characterized [5]. A microwave cavity similar to the one described in [6] has also been constructed and characterized with results as expected. The CsF-1 clock will be used, among other purposes, to provide accuracy information to the Atomic Time Scale of CENAM [7].

In Section 2 we discuss the characteristics of Light sources, the method we used to frequency stabilize the diode lasers, and optics configuration to prepare the light to feed the MOT. Section three is devoted to discuss the main characteristics of the MOT, its operational parameters, measurement of trapped Cs

atoms, temperature measurements, magnetic field gradient, among other parameters. In Section 4 we discuss the mechanical part of the CsF-1, like: flight region, vacuum tube, C-field coil, magnetic shielding and detection region. Finally, in Section 5 we discuss the performance characterization of Sapphire oscillators designed to be used as local microwave source for the CsF-1 and the method to frequency lock it to the clock transition.

2. LIGHT SOURCES AND OPTICS

The development of the thermal Cs beam optically pumped clock, the CsOP-1 clock, included DBR type diode lasers as light sources. DBR lasers used on the CsOP-1, emitting at 852 nm with 5 mW, have a spectral linewidth of 1 MHz. It is important to mention that such linewidth is narrow enough to operate an optically pumped thermal Cs beam clock without the necessity to include extended cavities to reduce the spectral linewidth as is reported in [2]. In Fig. 1 it is shown the resonance spectrum of the Cs D2 line using our DBR lasers.

As can be appreciated, the signal-to-noise ratio is similar to that obtained with extended cavity diode lasers, and also the sharpness of peaks seems to be not strength limited by the laser linewidth. In Fig. 2 we show results obtained when the frequency stability of lasers is measured using the beat signal between two DBR lasers frequency stabilized to the Cs D2 line by two different methods. Absence of extended cavity makes much simpler and robust the optical system of a clock, characteristics greatly appreciated when a clock is operated routinely.

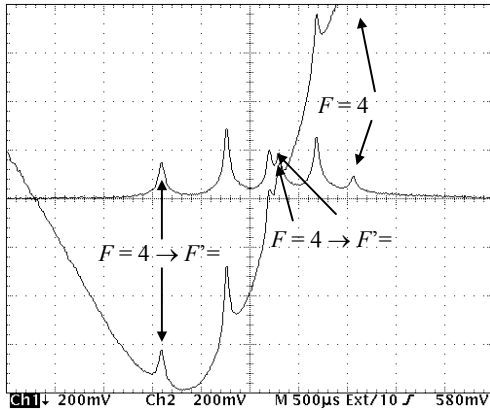


Fig. 1 Resonant spectrum of the Cs D2 line with and without Doppler well obtained with DBR diode lasers.

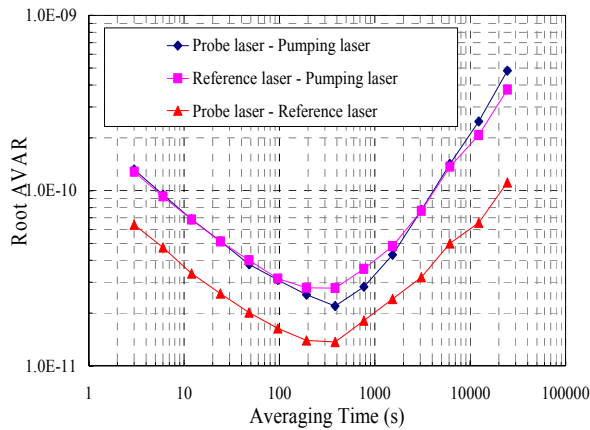


Fig. 2 Allan variance corresponding to the frequency differences between a pair of lasers.

Because of the good results obtained with DBR diode lasers on the CsOP-1 development, the optical part of the Magneto-Optical Trapp (MOT) of the CENAM fountain clock, the CsF-1, was also designed and integrated using DBR lasers as light sources. Fig. 3 shows the schematic of the MOT optical system. A DBR laser, 5 mW @ 852 nm, is used as master laser. It is frequency stabilized to the cyclic transition $F = 4 \rightarrow F' = 5$ by saturation spectroscopy. A double pass through two Acusto-Optic Modulators (AOMs), with cat eye configuration, is used to shift the color of the master laser beam to the red respect to the cyclic transition by around 12 MHz. Once the light of the master laser is red shifted a second laser, 50 mW @ 852 nm, referred as slave laser, is frequency stabilized to the master by the light injection technique. Because the cross section of the slave laser beam is pretty round most of its light can be used to feed it into the

MOT making an efficient use of its light. In Section 3 the mechanical design of the MOT and also results of its characterization is presented and discussed.

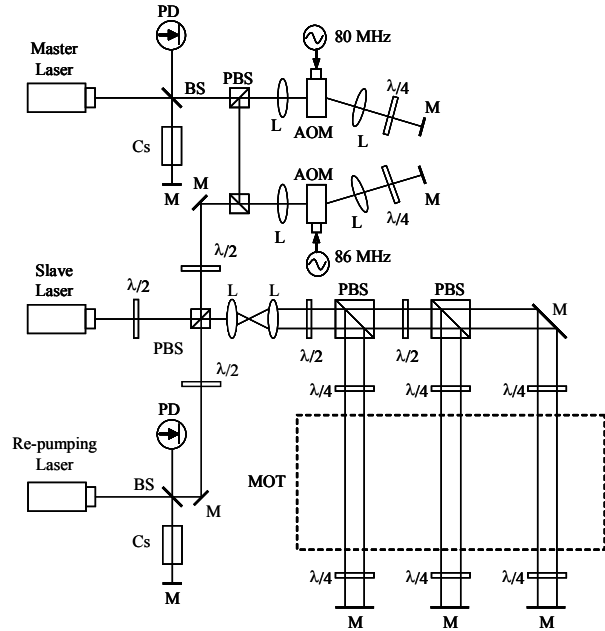


Fig. 3 Setup of the MOT optical system, where M is a mirror, $\lambda/4$ is a $1/4$ wave plate, $\lambda/2$ is a $1/2$ wave plate, BS is a beam splitter, PBS is a polarized beam splitter, AOM is an acousto-optic modulator, L is a lens and PD is a photo detector.

In Fig. 4 we show a schematic of the optical system for the full operation of the clock. In this case only one DBF laser is used to operate the entire optical system (except by the repumping and detection laser beams). The DBF laser used as single light source has an output power around 150 mW, emits at 852 nm when it is operated around the room temperature and its spectral linewidth is close to 1 MHz (similar to the one of the DBR lasers mentioned previously in this section) without the necessity of use of extended cavities. In [8] the results of comparison between a DBR laser and a DBF lasers are reported. Results obtained show a similar performance to those obtained with DBR lasers when used to make a Cs D2 spectroscopy as well as when they are frequency stabilized to that line. In order to achieve an efficient use of the DBF laser light it is first red shifted by around 165 MHz using a double pass through an AOM in cat eye configuration. After it is red shifted, a small portion of light is taken to achieve saturation spectroscopy on the Cs D2 line and frequency stabilization of the laser at the cyclic transition. With these approach, around 100 mW of frequency stabilized light is

obtained, the beam is then divided in two parts with the same intensity, one part is blue frequency shifted by 153 MHz to be used, previously divided, as the horizontal beams on the MOT. The second beam is divided in two in order to obtain the vertical beams. Of course, the vertical down beam is blue shifted by 165 MHz - $\delta/2$ MHz and the vertical up is blue shifted by 165 MHz + $\delta/2$ MHz. When δ is 0 MHz the trapping condition on the MOT is obtained. On the other hand, when $\delta \neq 0$ the moving molasses condition is obtained in order to push up the atoms against gravity.

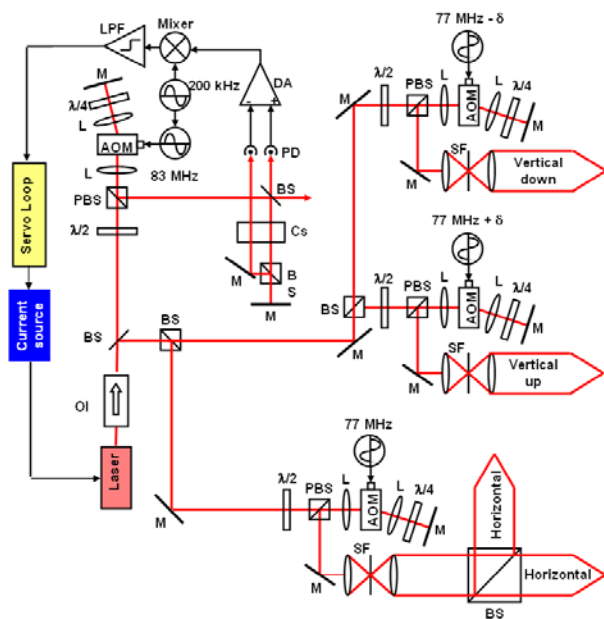


Fig. 4 Schematic of the optical system for the CsF-1 clock is presented. A single DBF laser is used as light source to operate the entire optical part of the CsF-1 MOT (except for the repumping and detection laser beams).

3. MECHANICAL PART OF THE MOT

The mechanical part of the CsF-1 MOT consists of a stainless steel sphere of 15 cm in diameter with twelve ports, six of them used to feed the laser beams, four in the horizontal plane and two in the vertical axis. The rest of the ports are used for the vacuum system, photo detectors, vacuum gauges, and CCD cameras. The Cs reservoir is connected to the sphere using the vacuum port. Optical windows are attached on ports used to pass through them the laser light or the atoms fluorescence. Windows are coated in both faces with an antireflection film for 852 nm obtaining a transmittance coefficient bigger than 99 %. With this excellent transmittance

coefficient a good balance of laser beam intensities inside the MOT is obtained. A $\sigma^+\sigma^-$ light polarization is used to operate the MOT. A $\lambda/4$ wave plate is used in the front of each window where a laser beam passes in order to properly circular polarize the laser beams. For each of the three axes, the cooling laser beams are feed through one window and back reflected through the second by a mirror. In Fig. 5 it is shown a picture of the stainless steel sphere of the MOT.

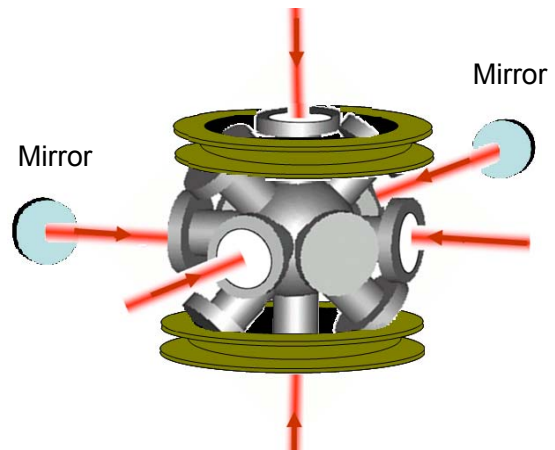


Fig. 5 MOT stainless steel sphere with anti-Helmholtz coils.

Two coils in anti-Helmholtz configuration are used to create a magnetic field gradient of few Gauss per centimeter at the center of the MOT. The radii of the coils is 15 cm with 50 turns each, an electric current of around 1 A is needed to operate them. The operation of the MOT has been characterized and results were reported in [4], however we will comment here some results of its characterization. Number of trapped atoms of course depends of several MOT parameters like: intensity of the laser beams, frequency red shifting, diameter of the laser beams, magnetic field gradient, among others. When operational parameters are properly adjusted we found in the MOT up to 6×10^7 trapped atoms. In Figs. 6 and 7 are shown the measurement results of the number of trapped atoms in the MOT when diameter, intensity and detuning of the laser beams are changed. In Fig. 8 the number of trapped atoms as function of the magnetic field gradient is shown. These results are in good agreement with previous results reported by other groups [9]. In Fig. 9 is shown a time of flight (TOF) signal obtained at 1 cm below the center of the MOT in order to preliminary

estimate the temperature in the MOT. TOF signal corresponds to a temperature of 30 μ K. TOF signal for longer trajectory is needed in order to better estimate temperature in the MOT. In any case, it is convenient to mention that when these temperature results were obtained the MOT parameters were not optimized to have the lowest possible temperature in the MOT. We estimate that a temperature of around 5 μ K can be obtained by carefully adjusting the MOT operational parameters for that purpose.

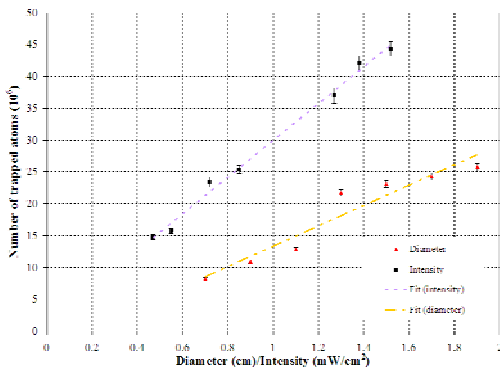


Fig. 6 Measurements of the number of trapped Cs atoms in the CENAM's MOT as a function of the intensity and diameter of the cooling beams, with a magnetic field gradient of 5.3×10^{-4} T/cm and 12 MHz red shift.

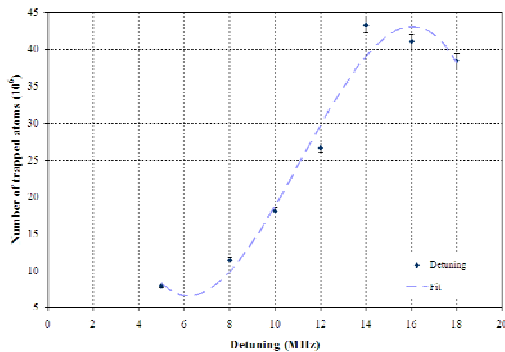


Fig. 7 Number of trapped Cs atoms in the CENAM's MOT as a function of laser detuning, with a diameter of laser cooling beams of 1.9 cm, intensity of cooling beams of 1.5 mW/cm², and a magnetic field gradient of 5.3×10^{-4} T/cm.

4. FLIGHT REGION

The flight region of the CsF-1 consists of the vacuum tank, the magnetic shield, the microwave cavities and the C-field coil. The vacuum tank of the flight region is currently under development, it is made of copper. A magnetic shield was constructed;

three μ -metal concentric cylinders form it. The most internal cylinder has 340 mm in diameter and 656 cm high. Inside the magnetic shield is the flight tube consisting of a cylindrical vacuum chamber, made of copper with 12 cm internal diameter, 13 cm external diameter and 500 mm high. The C-field coil is located on the outside face of the flight tube. The microwave cavity design is similar to the cavity used at the PTB atomic fountain, CSF1 [6]. It is a cylindrical cavity with a TE011 mode in the magnetic field oscillations. This mode exhibits a high intrinsic quality factor, implying a small variation of the field phase with radial position in the cavity. The Fig. 10 shows a schematic of the CsF-1 atomic fountain flight region. In Figs. 11 and 12 it is shown a numerical calculation of the central Ramsey fringes expected with this CsF-1 geometry.

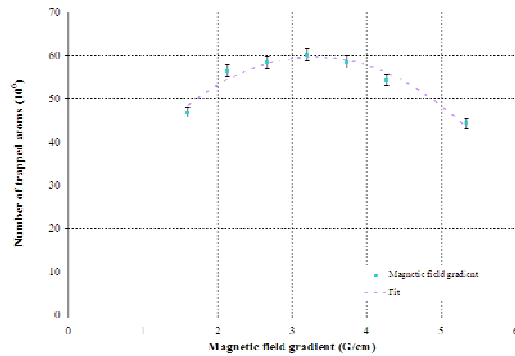


Fig. 8 Number of trapped Cs atoms in the CENAMs MOT as a function of the magnetic field gradient. Diameter of the cooling laser beams was 1.9 cm, laser detuning 14 MHz, and intensity of cooling beams 1.5 mW/cm².

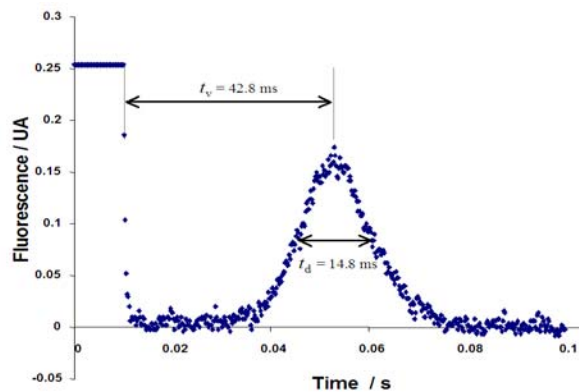


Fig. 9 Time of Flight (TOF) signal obtained at 1 cm below the center of the MOT in order to preliminary estimate the temperature in the MOT. TOF signal corresponds to a temperature of 30 μ K.

5. LOCAL OSCILLATOR

With the objective to have a very good frequency stability for short time on the CsF-1 microwave local oscillator, a sapphire whispering gallery resonator (WGR) oscillator has been developed at CENAM [5], [10], [11]. This type of oscillators offer a much lower phase noise level compared to that of the widely used microwave synthesizers based on quartz oscillators and frequency multiplication approach. In this section we present preliminary results achieved on the C- and X-band ultra low phase noise WGR oscillators.

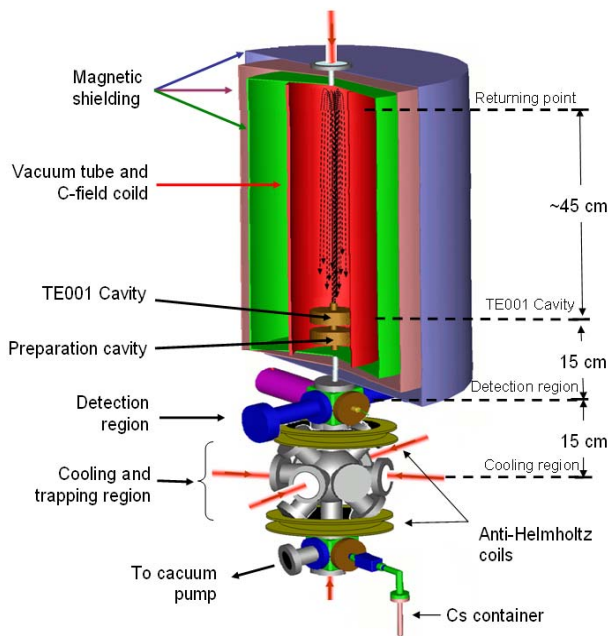


Fig. 10 The CsF-1 mechanical design. An Ion vacuum pump (not indicated in the schematic) is located in the upper part to improve the vacuum in the flight region. The vacuum tank of the flight region is made of copper and its outside face is used to turn around the C-field coil.

The lowest phase noise microwave oscillators are built with the use of combined frequency stabilization technique. This technique assumes that the same WGR is used both as a feedback resonator in the main oscillator loop and as a dispersive element of the frequency discriminator (FD) which together with some additional electronics forms an additional phase noise suppression system.

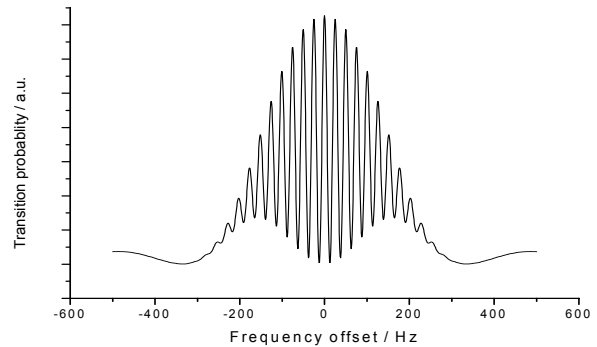


Fig. 11 Numerical calculation of the Ramsey fringes expected for the CsF-1

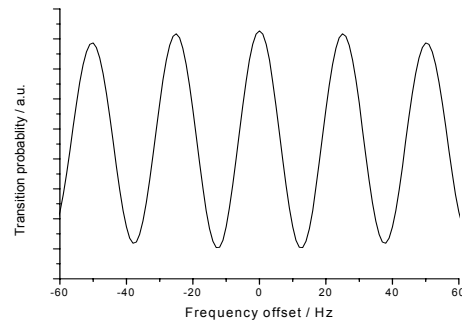


Fig. 12 Central fringes of the CsF-1 Ramsey pattern.

The most efficient FDs can be implemented using the properties of the wave that reflects from WGR. Commonly, for the reflected signal extraction a ferrite microwave circulator is used. An alternative approach for the reflected signal extraction is the excitation of a WGR in a traveling wave (TW) regimen. The basic TW resonant structure suitable for a microwave oscillator application is also known as a traveling wave directional filter (TWDF). This type of filters have a four port configuration and can be implemented exciting a microwave resonator using orthogonal probes fed by 3-dB quadrature directional couplers as it is shown in Fig. 13. A particular property of the TWDF is that its port 1 to port 2 transmission coefficient has a reflection-like frequency response, while the transmission coefficient from port 1 to port 3 is equivalent to that one of the conventional standing wave resonator coupled in transmission. Hence, a TWDF allows building both an oscillator loop and a high efficiency FD avoiding the microwave circulator utilization. Another advantage of the TWDF is that the last one on contrast to the conventional standing wave resonator, it is a matched device and its impedance does not depend on the resonator coupling that in its

turn is very favorable for a loop amplifier performance. For the experimental TWDF implementation, the sapphire WGR with the same dimensions as in the case of reflection oscillator design has been used. For a proper TW regimen realization the WGR has been excited on $WGH_{7,1,1}$ -mode according to the schematic shown in Fig. 13 (see also Fig. 14). To feed the excitation and analysis probes, the 3-dB branch-line couplers fabricated on Taconic RF-60 substrate have been used.

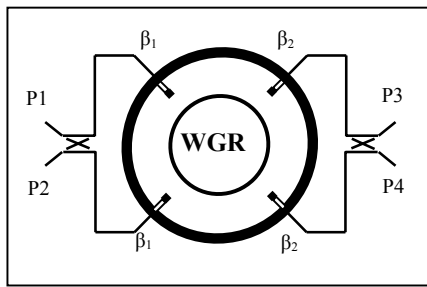


Fig. 13 Sapphire 4-port TW directional filter.

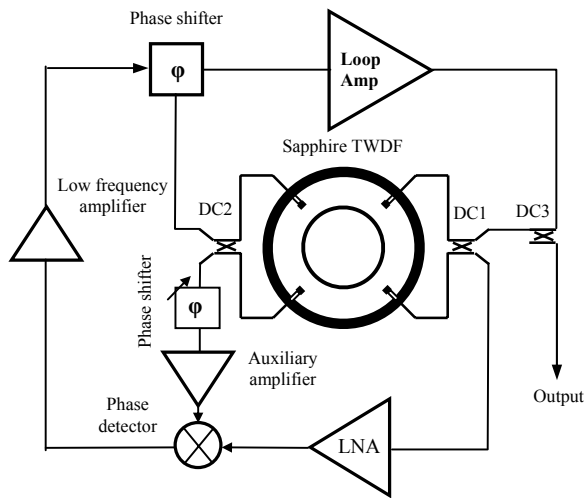


Fig. 14 TWDF based microwave oscillator with combined frequency stabilization.

A phase noise of the free running TW oscillator has been measured analyzing the signal at the phase detector output. For these measurements the WGR coupling coefficient β has been adjusted very close to the unity that permitting to obtain a carrier suppression level of about 40 dB and thus maintaining the LNA operating in the small signal regimen with $P_{in} < -20$ dBm. According to our

measurements reported in a noise floor of the designed system should be around -180 dBc/Hz and for the mentioned input power level its $1/f$ -noise corner frequency should be lower than 300 Hz. The measured spectral density of the frequency fluctuations of the free-running oscillator is shown in Fig. 15. According to these measurements, at 1 kHz offset frequency the oscillator's frequency noise resulted to be $S_f(1\text{kHz}) = 8 \cdot 10^{-7} \text{ Hz}^2/\text{Hz}$, that makes the SSB oscillator phase noise to be $L(1 \text{ kHz}) = -124 \text{ dBc/Hz}$. The measured free-running TW oscillator phase noise can be considered to be very low especially taking into account its elevated output power. It is important to mention that such a low initial oscillator phase noise level makes easier the implementation of the noise suppression system. In particular it permits to reduce the gain of the noise suppression loop thus improving the entire system stability.

Finally we would like to give a theoretical estimation of the designed oscillator phase noise limit. As it has been mentioned in a large number of works, the phase noise of an oscillator in combination with frequency stabilization is basically limited by the FD noise floor. In its turn, our configuration the FD contains two main noise contributors, the LNA and the phase detector. Thus, the oscillator phase noise limit imposed by the FD noise floor can be defined from the following Eq. (1):

$$L_{\phi}^{FD}(f_m) = [kT_K NF(f_m)/2P_{inc}] \times T_0^{-2} \times (B_0/f_m)^2, \quad (1)$$

where k – a Boltzmann constant; T_K – temperature in Kelvin; P_{inc} – microwave power at the FD input; $B_0 = f/2Q_0$; f_m – an offset frequency; T_0 – parameter describing the FD efficiency; $NF(f_m)$ – the overall noise figure of the FD microwave circuitry given by:

$$NF(f_m) = NF_{LNA}(f_m) + \frac{NF_{PD}(f_m) - 1}{G_{LNA}}, \quad (2)$$

where $N_{LNA}(f_m)$ – the LNA noise figure; $N_{PD}(f_m)$ – the phase detector noise figure and G_{LNA} – the LNA gain. In order to make an estimation of the oscillator phase noise let us assume: $P_{inc} = 150 \text{ mW}$, $f = 4.6 \text{ GHz}$, $Q_0 = 300,000$, $N_{LNA} = 2 \text{ dB}$, $N_{PD} = 20 \text{ dB}$, $G_{LNA} = 33 \text{ dB}$, substituting these parameters in Eqs. (1) and (2), we obtain: $L_{\phi}^{FD}(1\text{kHz}) = -165 \text{ dBc/Hz}$. Considering the phase noise estimation, it is expected that the oscillator should have its noise characteristics comparable to those reported in for X-band 0.4 W oscillators. In order to accomplish the experimental phase noise characterization, a second

oscillator and a phase noise measurement setup are currently being constructed. The results of the comparison between these two oscillators will be reported shortly.

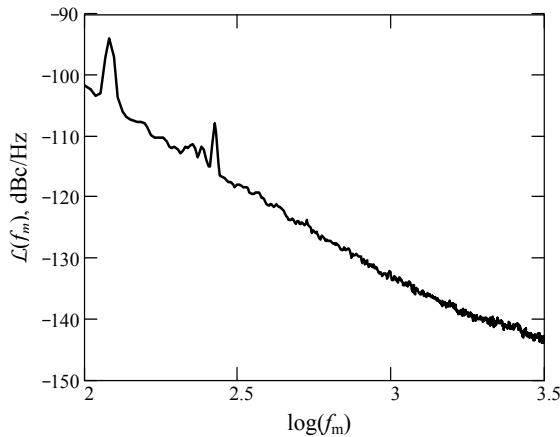


Fig. 15 Measured phase noise spectrum of the 1 MHz beat note between two 4.79 and 4.80 GHz WGR oscillators.

4. CONCLUSIONS

The Centro Nacional de Metrología, CENAM, is currently developing a Cs fountain frequency Standard, which is referred as the CsF-1 clock. A solitary DBF laser will be used to operate the entire optical part of the fountain (with the exception of the repumping laser). The DBF laser has a spectral linewidth of 1 MHz without the necessity of extended cavity. This will make the optical part of the CsF-1 much simpler, compact and robust, characteristics greatly appreciated when a clock is operated routinely. A configuration of four laser beams in the horizontal plane and two laser beams in the vertical axis is used along with a $\sigma^+\sigma^-$ light polarization. The returning point of the atoms above the cavity will be around 45 cm. A novel design of a Sapphire microwave oscillator has been developed and integrated with the aim to be used as local oscillator on the CsF-1 clock, its characterization as been achieved with good results. This sapphire oscillator will operate at room temperature. When writing this article the vacuum tank of the flight region is under construction. This primary frequency standard is developed with the aim to contribute to the BIPM with measurements for frequency correction to the EAL time scale. Finally we would like to mention that it is expected to obtain the first Ramsey signal of the CsF-1 by the end of the 2008 year.

REFERENCES

- [1] S. López et al, "High accuracy evaluation of CENAM's primary frequency standard: second order Doppler shift", Proc of the CPEM 2002, pp. 454-455.
- [2] S. López et al, "Mejoras al reloj atómico de bombeo óptico del CENAM", this conference.
- [3] J. M. López-Romero et al, "Cesium-133 Magneto Optical Trap at CENAM", Proc. of the CPEM 2002, pp. 466-457.
- [4] M. Talavera et al, "Accurate absolute measurement of trapped Cs atoms in a MOT", Revista Mexicana de Física **53**(5), pp. 358- 365
- [5] N. Shtin et al, "Development of ultra low phase noise microwave oscillators at CENAM", Proc of the 2008 European Frequency and Time Forum, Toulouse, France, April, 2008.
N. Shtin et al, "Desarrollo de osciladores de zafiro en el CENAM", this conference.
- [6] R. Schroder et al, "Design and realization of the microwave cavity in the PTB caesium atomic fountain clock CSF1", Ultrasonics, Ferroelectrics and Frequency Control, IEEE Transactions on Volume 49, Issue 3, Mar 2002 Page(s):383 - 392
- [7] J. M. López-Romero et al, "Establishment of the SIM time scale", this conference.
- [8] E. de Carlos L. et al, "Estudio de la emisión espectral de láseres semiconductores tipo DBF", this conference.
- [9] K. Lindquist, M. Stephens, and C. Wieman, "Experimental and theoretical study of the vapor-cell Zeeman optical trap", *Physical Review A* **46** (1992) 4082.
- [10] N. Shtin, J. M. Lopez Romero and E. Prokhorov, "Novel Sapphire Directional Filters for Ultra Low Phase Noise Applications," in proc. 49th IEEE MWSCAS, 2006, pp. 42-46.
- [11] N. A. Shtin, J. M. Lopez Romero and E. Prokhorov, "Design and Performance of Ultra Low Phase Noise Reflection Whispering Gallery Resonator Oscillator," Microwave and Optical Technology Letters, Vol. 49, No 8, pp. 2026-2030, 2007.